Ultrastable performance of an underground-based laser interferometer observatory for gravitational waves

Shuichi Sato,[1,*] Shinji Miyoki,[2] Souichi Telada,[3] Daisuke Tatsumi,[1] Akito Araya,[4] Masatake Ohashi,[2] Yoji Totsuka,[5,†] Mitsuhiro Fukushima,[1] and Masa-Katsu Fujimoto[1]

(LISM Collaboration)

[1]*National Astronomical Observatory of Japan, 2-21-1 Osawa, Mitaka, Tokyo 181-8588, Japan*
[2]*Institute for Cosmic Ray Research, The University of Tokyo, 5-1-5, Kashiwanoha, Kashiwa, Chiba 277-8582, Japan*
[3]*National Institute of Advanced Industrial Science and Technology, 1-1-1 Umezono, Tsukuba, Ibaraki 305-8563, Japan*
[4]*Earthquake Research Institute, The University of Tokyo, 1-1-1, Yayoi, Bunkyo-ku, Tokyo 113-0032, Japan*
[5]*Kamioka Observatory, Institute for Cosmic Ray Research, The University of Tokyo, Higashi-Mozumi, Kamioka, Yoshiki-gun, Gifu 506-1205, Japan*

(Received 28 January 2004; published 28 May 2004)

In order to detect the rare astrophysical events that generate gravitational wave (GW) radiation, a sufficient stability is required for GW antennas to allow long-term observation. In practice, seismic excitation is one of the most common disturbances effecting the stable operation of suspended-mirror laser interferometers. A straightforward means to allow a more stable operation is therefore to locate the antenna, the ''observatory,'' at a ''quiet'' site. A laser interferometer gravitational wave antenna with a baseline length of 20 m (LISM) was developed at a site 1000 m underground, near Kamioka, Japan. This project was a unique demonstration of a prototype laser interferometer for gravitational wave observation located underground. The extremely stable environment is the prime motivation for going underground. In this paper, the demonstrated ultrastable operation of the interferometer and a well-maintained antenna sensitivity are reported.

DOI: 10.1103/PhysRevD.69.102005 PACS number(s): 95.55.Ym, 04.80.Nn, 95.85.Sz

I. INTRODUCTION

First-generation ground-based gravitational wave antennas [Laser Interferometer Gravitational Wave Observatory (LIGO-I) [1,2], VIRGO [3,4], GEO 600 [5–7], and TAMA 300 [8–10]] are expected to come on-line early in this decade as a global network searching for astrophysical gravitational wave (GW) radiation. At present, some of the detectors are already operating intermittently, hoping to observe the spacetime strain of the universe.

The aim of these international projects is to directly detect gravitational radiation, faint ripples in the spacetime fabric. There are several kinds of expected astrophysical sources, including chirping gravitational waves from inspiraling compact star binaries, burst signals from supernovae explosions, and the stochastic background radiation. The expected event rate of these sources is, however, quite low even if the uncertainty of the population estimate [11–13] is taken into account, so, to avoid missing these rare and faint signals, stable operation of the detector, keeping the duty cycle and the detector sensitivity high, and also keeping the data quality high are indispensable requirements for a gravitational wave observatory. In general, the technologies used in a laser interferometer are based on an ultrahigh precision measurement pursuing extremely high sensitivity, so the instruments are very sensitive to almost all kinds of noise, disturbances, and drifts. The noise source that most commonly disturbs stable operation of suspended-mirror laser interferometers is seismic excitation. The most promising solution for this problem is to avoid the source of these disturbances by selecting a quiet environment for a detector site.

The goal of this project (LISM, Laser Interferometer gravitational-wave Small observatory in a Mine) is to demonstrate stable operation of the laser interferometer and to obtain high-quality data for searching for gravitational waves at a well-suited observatory site.

The 20-m baseline laser interferometer was originally developed for various prototyping experiments [14–17] at the campus of The National Astronomical Observatory of Japan, in Mitaka, a suburb of Tokyo, from 1991 to 1998. In 1999, it was moved to the Kamioka mine in order to perform long-term, stable observations such as LISM. In this paper, the merit of going underground and the demonstrated stable operation of the antenna are reported. The results of data analysis and a GW search will appear as a separate article [18].

II. THE KAMIOKA SITE

Kamioka is in a mountainous area, about 220 km west of Tokyo. The observatory site is inside a mountain. The laboratory facility was built 1000 m underground beneath the top of the mountain, utilizing some of the tunnel network that was originally developed for commercial mining activity. This site is also well-known as the site for the Super-Kamiokande nucleon decay experiment [19] and other cosmic ray experiments, which all need a low-background environment deep underground. This site is the most probable

*Email address: sato.shuichi@nao.ac.jp
†Present address: High Energy Accelerator Research Organization (KEK), 1-1 Oho, Tsukuba, Ibaraki 305-0801, Japan.

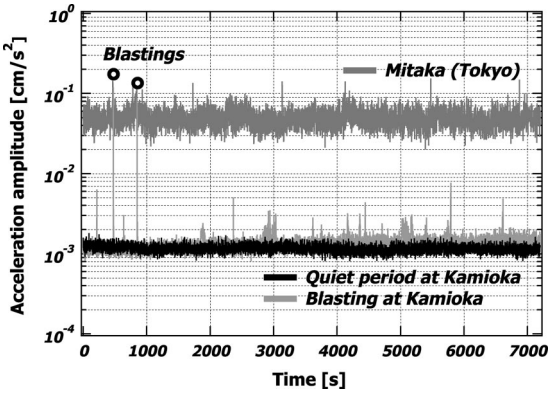

FIG. 1. The acceleration amplitude due to the seismic motion measured with accelerometers is shown as a function of time. The acceleration of the Tokyo site is typically greater than that of the Kamioka site by about two orders of magnitude. Two noise spikes around 500 and 900 sec are caused by blasting activity near the site. These noise spikes have a level almost comparable to the usual acceleration level of Tokyo.

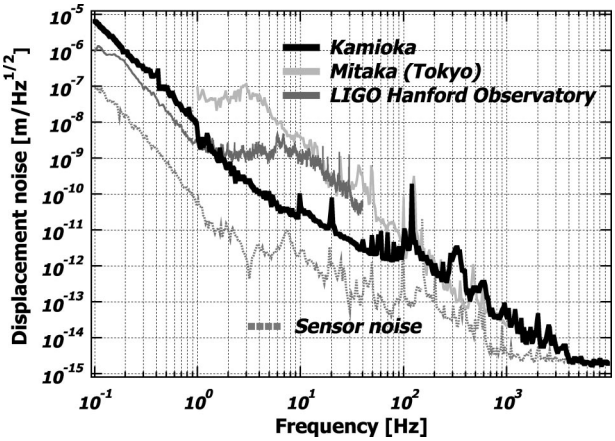

FIG. 2. The seismic noise of the site in the horizontal direction is shown in displacement as a function of the Fourier frequency. The difference in the low-frequency region below 100 Hz clearly shows the merit of the Kamioka underground site. The seismic displacement noise of LIGO Hanford Observatory (LHO), measured inside one of the station buildings [29], is shown as a reference. The frequency range of the LHO spectrum was limited by the bandwidth of the seismometer sensor.

candidate for the future Japanese full-scale gravitational wave antenna project (LCGT) [20,21].

The most decisive reason why Kamioka was selected as the detector site for LISM was that the seismic noise level in the underground facility is extremely low with few artificial seismic excitations. The quiet environment there is an overwhelming benefit for a suspended-mass laser interferometer because the stability of the system depends largely on the lack of seismic and other environmental disturbances. For the laser interferometer once technical noises are suppressed, the spectral sensitivity at the lowest-frequency region (typically below a few 10 Hz) is expected to be limited by the seismic noise even after the attenuation by the vibration isolation systems, so low-level seismic noise is quite important in this frequency region. In addition, slow motion of the ground below 1 Hz, including microseismic noise, also plays an important role for stable operation of laser interferometer. The rms value of the seismic displacement in this frequency region affects lock acquisition, stability, and robustness of the lock. This is because the suspension systems, which have an eigenfrequency of about 1 Hz, cannot be expected to have sufficient isolation at and below that frequency.

The typical seismic acceleration is plotted as a function of time at the Kamioka site in comparison with that of Tokyo in Fig. 1. The rms value of acceleration at the LISM site is about 100 times smaller than that at the Tokyo site, which is almost comparable with the transient excitations generated by blasting activities of mining nearby. The displacement noise power spectrum of seismic motion is shown in Fig. 2. The seismic motion is smaller than that of Tokyo by two to three orders of magnitude in the low-frequency region. The fact that seismic motion is extremely small at lower frequencies (below 1 Hz typically) is due to the fact that Kamioka is located in a relatively quiet region of the Japan islands while the low seismic noise at observational frequencies is due to the fact that the laboratory site is deep underground, 1000 m from the surface, so the seismic motion is strongly damped in the high-frequency region.

In addition, there is a much smaller temperature variation in the underground cave than at the surface, as shown in Fig. 3. As the variation was so small, no temperature control system was employed for the laboratory containing the LISM antenna. This was better than having an active temperature control system. The temperature stability at the site was considerably better than that at the surface-based TAMA 300 site, which is air conditioned. The temperature variation (drift) in the laboratory was about 0.01 °C each day in the absence of operators. Human presence was the most significant heat and moisture source in this environment. Owing to the excellent temperature stability, the drift of the control loops, the fluctuations in the frequency of laser light, the

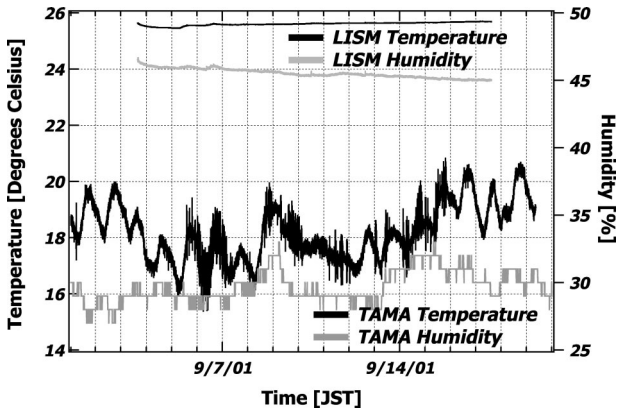

FIG. 3. The temperature and humidity variation in the LISM laboratory in comparison with that in the TAMA 300 site. The variations of the LISM site were almost flat, showing 0.01 degree/day and 0.08%/day for temperature and humidity variation, respectively. In addition, there were no apparent daily variation, and the trend over several days was caused by the change in the weather, which was clearly seen in the TAMA 300 site data even though air conditioning was used.

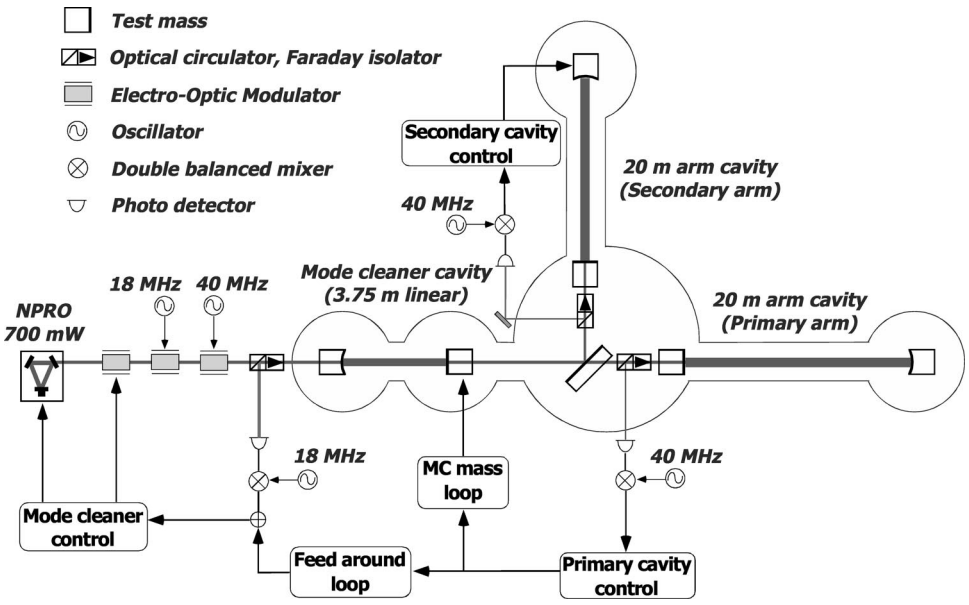

FIG. 4. The schematic of the optical layout and control scheme of the LISM interferometer. The main interferometer employs a so-called locked Fabry-Perot system, with MISER as a laser source and a linear-type mode cleaner optical cavity. The laser frequency was stabilized by using the mode cleaner and primary cavity as a frequency reference. The multistage stabilization scheme was used for this purpose with a bandwidth over 1.2 MHz. The output signal that should contain gravitational signals was extracted from the secondary control loop.

beam pointing, the alignments of optics, and the variation of other parameters were expected to be sufficiently suppressed. Another merit of the underground site should also be mentioned. There is less influence from bad weather, winds, high wave, typhoon, and so on, which often disrupt the operation of the TAMA 300 interferometer.

In view of these aspects, the underground environment at Kamioka is expected to be very suitable for stable long-term operation of a laser interferometer as a gravitational wave observatory.

III. INTERFEROMETER CONFIGURATION

A. Optical configuration

The optical layout of LISM shown in Fig. 4 is based on a Michelson-type interferometer whose arms contain 20 m Fabry-Perot optical cavities to enhance the effect of gravitational waves, a so-called locked Fabry-Perot interferometer [22]. The frequency of the laser was stabilized by using the primary cavity as a frequency reference. In other words, the laser frequency was a measure of the spacetime curvature along the direction of the primary arm. By measuring the variation of the secondary cavity length, which is a reference now of the curvature of spacetime along the perpendicular arm cavity direction, it is possible to sense the differential strain generated by a gravitational wave.

Both Fabry-Perot arm cavities had a finesse of about 25 000, which corresponds to a cavity pole frequency of 150 Hz. Despite the short arm length, the photon storage time was increased to 1 msec by the high finesse. A commercial Nd:YAG (yttrium aluminum garnet) laser running at 1064 nm, MISER (Light Wave Electronics Co., Ltd.), was used as a light source which yielded an output power of 700 mW. The interferometer is equipped with another suspended Fabry-Perot cavity, the so-called mode cleaner (MC), in front of the main interferometer. It is quite important for the spatial filtering of the incoming laser light, and as a first stage reference for the laser frequency stabilization. The length of the mode cleaner was chosen to be 3.75 m to have a free spectral range (FSR) of 40 MHz, which enables the 40 MHz rf-phase modulation sidebands to pass through it (sideband transmission).

Test masses for the interferometer are made of monolithic fused silica substrates, whose dimensions are 50 mm in diameter and 60 mm in thickness. The surfaces are superpolished and coated with high-quality dielectric multilayer films by ion beam sputtering. The resulting mirrors had an intensity reflection of 0.999 875 and a total loss of 27 ppm [23]. The test masses of the main interferometer and the mode cleaner mirrors were suspended as double-stage pendulums in order to isolate them from seismic noise. The pendulum resonances at the eigenfrequencies (pendulum modes) were suppressed by using eddy current damping with permanent magnets attached to the magnet holder surrounding intermediate masses. For control, four small permanent magnets were glued onto the back of each mirror. Together with coils fixed on a pendulum cage, the coil-magnet actuators control the mirror position along the beam axis.

The main interferometer and the mode cleaner are housed in vacuum chambers connected by 200-mm-diam vacuum tubes. During the observation, the vacuum was 10^{-4} Pa and was maintained by two ion pumps, as they are free from mechanical vibration.

In order to control the length degrees of freedom of the cavities, a Pound-Drever-Hall technique was used [24]. The error signal of the primary cavity was fed back to the laser frequency via both the MC cavity and a feed-around path [25]. The control bandwidth of the MC loop was increased to 1.2 MHz, having a loop gain of 80 dB at 1 kHz, and that of the primary-cavity loop was 200 kHz, with a loop gain of 50 dB at 1 kHz. Owing to this wide-band, high-gain frequency stabilization control, frequency noise was sufficiently suppressed so as not to contribute to the resulting noise curve, even though the common mode rejection by optical recombination at the beam splitter, as conventionally used, was not employed here. The information of the length of the second-

ary cavity, which should contain the gravitational wave signals, was taken from the feedback of the control loop and recorded.

B. Automatic lock-acquisition system

In order to perform long-term operation of the laser interferometer, remote control and/or automated lock maintenance systems are required for a gravitational wave observatory. This reduces the work load for the operators, and also minimizes the disturbances caused by the work of the operations. For the LISM interferometer, a stand-alone automation system was developed. On detecting the loss of lock, the lock-acquisition sequence was automatically performed to regain the operational mode. Owing to this system, the operator could simply monitor the interferometer condition from outside the mine. These systems are based on hardware control using a TTL digital signal. The state of the interferometer was judged by monitoring the optical power of the transmission and/or the reflection of the Fabry-Perot cavities. This information was communicated as a TTL signal, to engage, switch, and change the characteristics of the analog control loops via appropriate digital circuitry that provides sequential timing signals. One aspect which is different from that at the Tokyo site is that the motion of the suspended mirrors is so small that it takes a long time for the cavities to pass through one free spectral range (FSR). In other words, as the Fabry-Perot cavities have a resonance flash so infrequently, they cannot acquire lock in a reasonable time by themselves. Without an automatic lock-acquisition system, i.e., if the control systems are left waiting for self relock, it typically took a day to reacquire lock and become operational after an unlock of the interferometer. This will be mentioned again and justified later in the result section.

For quick lock acquisition, the wavelength of the laser light or the length of the cavities was actively swept by injecting sweeping signals to the feedback points of the control loops until the cavities acquired lock. The sweeping was performed softly and slowly enough that the control system could acquire lock even with the high-finesse arm cavities. Once one of the cavities was locked, the sequential switching processes were initiated. The main functions of these processes were the change of the control servo (servo gain increase, dc gain booster, etc.), optical power increase (reduced power was used for lock acquisition), and switching of the circuits for sweeping-signal injection. Using this system, the whole interferometer became operational within 100 sec typically. Once the systems were properly tuned, this automated lock acquisition system worked very reliably, and the failure rate of the relock acquisition sequence was very low, which strongly contributed to the excellent duty cycle.

IV. INTERFEROMETER SENSITIVITY AND NOISE BUDGET

The noise equivalent spectral sensitivity curve of the LISM interferometer is shown in Fig. 5, together with identified noise sources. After much effort to reduce noise, the detector achieved a floor sensitivity of $1.3\times10^{-18}\mathrm{m}/\sqrt{\mathrm{Hz}}$ around 800 Hz in displacement, which corresponds to $6\times10^{-20}/\sqrt{\mathrm{Hz}}$ in strain. Noise sources that limited the detector sensitivity were to a large part identified in a wide frequency range.

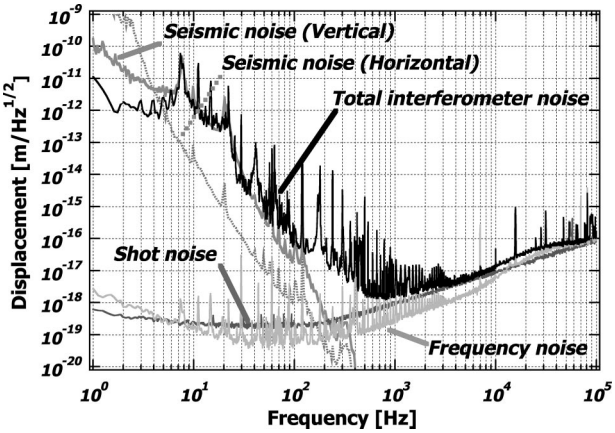

FIG. 5. The noise equivalent detector sensitivity is shown in displacement together with identified noise sources that were limiting the sensitivity. The frequency noise was suppressed well and optical shot noise was the dominant contribution in the higher-frequency region above 1 kHz. In the lower-frequency region below 100 Hz, seismic noise in the vertical direction which couples through the suspension system exceeded direct horizontal seismic noise and had a significant influence on the detector sensitivity.

For the high-frequency range above 1 kHz, photon shot noise was dominant, corresponding to the input light power to the secondary cavity of 35 mW. The arm cavities are designed to be critically coupled so that only the rf modulation sidebands are reflected to the detector. In this regime, the shot-noise limited sensitivity is maximized in the limit where the rf sideband power goes to zero. However, there is some amount of carrier reflection due to finite optical losses of the optics and mismatch of reflectivity between the two cavity mirrors. In the regime where the detected power is dominated by the carrier, the shot-noise limited sensitivity can be improved by increasing the amplitude of the rf sidebands until the sideband power dominates. Therefore, the rf sideband power was adjusted to optimize the signal-to-noise ratio.

For the lower frequencies, below several hundred Hz, the seismic noise was dominant. The calculated seismic noise level in the horizontal direction, using the measured seismic noise spectrum and the calculated transfer function of the suspension system, showed no contribution to the interferometer sensitivity curve in the observational band. On the other hand, the estimated contribution of the vertical seismic noise, which can be converted to horizontal motion via vertical-horizontal cross coupling of the suspension system, could explain well a resonance structure around a few tens of hertz. In the lowest-frequency region, below 6 Hz, the noise curve of the interferometer is below the expectation of seismic noise contributions. This is thought to be an effect of common mode suppression. The velocity of the elastic wave, which is a function of the elasticity modulus and matter density, at this location is rather fast, so the wavelength of the

seismic motion at low frequency is presumed to be comparable to the 20 m arm length. Therefore, in this low-frequency region, the two test masses composing the Fabry-Perot cavity are considered to be moving together, so there is less relative displacement between them. This is more evidence that the ground underneath the Kamioka site is stiff and firm, where the primary wave velocity is the order of 5500 m/s. The accumulated displacement between two test masses was calculated to be of the order of 10^{-10} m, by integrating the noise spectrum down to 0.1 Hz, which corresponds to an accumulated rms velocity on the order of 10^{-9} m/s. This means that the round-trip phase of the Fabry-Perot cavity changes very slowly, owing largely to the significant common mode rejection of displacement between the cavity mirrors. This is consistent with the fact that the antenna took one night to relock by itself if left as is. The excess noise between these two frequency regions (shot-noise limited high-frequency region and seismic-noise limited low-frequency region), around 100 Hz, was suspected to come from unwanted coupling through the suspension systems. There are several candidates for the source of noise which coupled through the suspension systems, and it is not clear which was the problem, however by improving the suspension system this noise was eliminated. Consequently, all the noise sources contributing to the interferometer sensitivity were fully identified as shot noise, seismic noise, and suspension-oriented noise.

V. OBSERVATION AND RESULTS

Several observational runs were performed from the beginning of 2000, with an accumulated observation time on the order of 3000 h. Of significance, 1000 h of data were taken in the summer of 2001 in coincidence with the TAMA 300 detector. The report on the development of the coincident analysis method and the results using LISM and TAMA 300 data will appear as an independent article elsewhere. In this paper, the achievement of ultrastable operation of a gravitational wave antenna and its importance are emphasized.

A. Tidal motion

During the operation of the interferometer, the Fabry-Perot cavities were controlled in length in order to keep them on resonance. In principle, the mismatch between cavity length and wavelength of the laser light is sensed and then fed back to their actuators via appropriate servo filters so that these feedback signals cancel the deviations. In other words, that feedback signal contains the information for the change of the cavity length together with the change of the wavelength of the laser light, which can be caused, for example, by temperature variation. The PZT actuator of the laser was used for a laser frequency tuning in the low-frequency region, so the feedback signals on the actuator for the primary cavity were converted to strain-equivalent quantities in Fig. 6. These variations include both the change of the cavity length itself and that of the wavelength of the laser light, and these two effects cannot be distinguished in principle. Although there is a large drift over several days in one direction, a tidal component was clearly seen on it. This shows that there is less seismic motion and environmental disturbances (for example temperature variations) than that which would screen the tidal strain components. The observed equivalent strain was separated into three components, namely long-term drift, noise, and tidal effects. The tidal component was calculated by tidal analysis software, BAYTAP-G [26], using the interferometer location (137.18°E,36.25°N) and the orientation. By fitting the data, the strain at the Kamioka site caused by tidal motion of the Earth was on the order of 10^{-8}, which was almost the same as the calculated value.

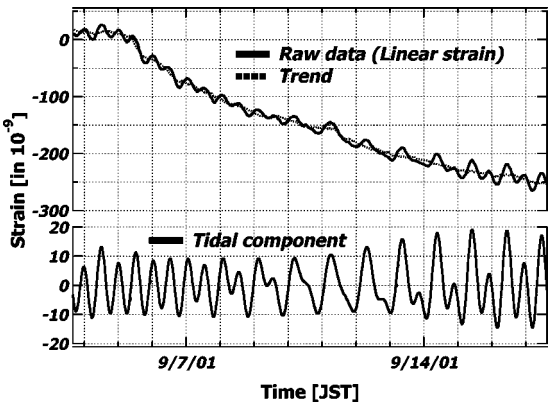

FIG. 6. The strain of the arm cavity relative to the primary cavity. Discontinuities of the raw data correspond to the cavity unlock. The tidal modulation components are clearly seen in the trend. The geophysical response at the site to the tidal force turned out to be on the order of 10^{-8}.

B. Operational stability

The operational status of the interferometer for one week from the two months of observational operation is shown in Fig. 7 with Japanese standard time (JST) on the horizontal axis. Three bars show the lock status of each of the three cavities: the mode cleaner, the primary, and the secondary cavities. Lock was lost a total of 12 times during this period;

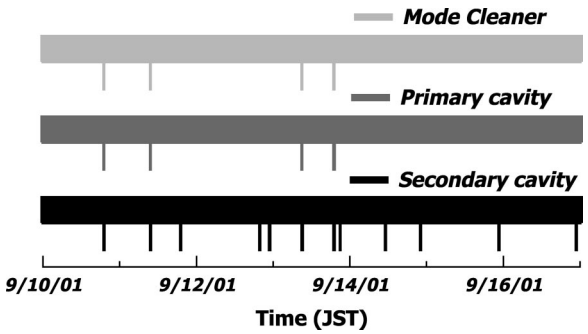

FIG. 7. The operational status of the three cavities of the interferometer is shown for a one-week period. Each bar shows ''operational status,'' the lines below the bars representing unlocks. There were 12 unlocks during this period, however there was no long unlock which significantly lowered the duty cycle of the antenna. The resulting duty cycle was 99.8%. Most of these unlocks were due to the impulsive seismic noise caused by blasting.

in 10 of these 12 times, the cause was blasting activity of the mining company. However, the interferometer typically became operational again after about 100 s (the shortest recovery occurred within a few seconds), and the resulting accumulated dead (loss) time was only 1440 sec during that 7 day period, so the antenna was operational 167.6 h out of the 168 h of total observation time in this period, which corresponds to a duty cycle of 99.8%. This is a tribute to the environmental stability of the site, and the automation systems. The blasting from the mining activities has been terminated in the mountain, so the frequency of the unlocks in the future observations will be significantly reduced, and longer stretches of lock are expected. Actually, the LISM detector had a record of 270 h of continuous operation in another observation period, when blasting was not being done.

C. Sensitivity stability

From the point of view of the observation of gravitational waves, the stability of the sensitivity and the data quality are all vital issues for searching for gravitational wave signals. There may, however, be requirements for the data quality that differ depending on the target GW signals and the analysis methods. There also are several ways to evaluate the spectral sensitivity, for example the spectrogram, which is sometimes used for a burst event search [27]. Here we adopt the expected binary range of a matched filtering analysis as an index to evaluate the spectrum sensitivity quantitatively. The binary range (R_B) is defined as follows [28] using the spectral sensitivity of the detector with assumed specific signal-to-noise ratio (SNR) value:

$$R_B = 4A\left[\int_0^{f_c} \frac{f^{-7/3}}{S_n(f)}\mathrm{d}f\right]^{1/2}, \tag{1}$$

$$A = \frac{T_\odot^{5/6} c}{\mathrm{SNR}}\left(\frac{5\mu}{96 M_\odot}\right)^{1/2}\left(\frac{M}{\pi^2 M_\odot}\right)^{1/3}. \tag{2}$$

Here, $S_n(f)$ is the noise power spectrum of the detector, c is the speed of light, $\mu = m_1 m_2 / M$ is the reduced mass, $M = m_1 + m_2$ is the total mass of the binary system, $T_\odot = (G/c^3) M_\odot$ is the solar time, and $M_\odot$ is the solar mass. The cutoff frequency was defined as $f_c = M_\odot/(6^{3/2}\pi M T_\odot)$ in this calculation. As the matched filtering analysis is performed over some Fourier frequency ranges defined by a particular cutoff frequency depending on the chirp mass, any change of spectral sensitivity in these frequency regions influences the results of this evaluation. An expected binary range for gravitational wave radiation from coalescence of equal mass binary systems is shown in Fig. 8 as a function of member star mass. This shows how far the detector can see the GW event with SNR=10. The detector was, for simplicity, assumed to be optimally oriented to the gravitational wave source both in direction and its radiation polarization. According to this result, LISM has a sensitivity to detect inspiraling gravitational waves from 1.4–1.4 $M_\odot$ neutron star coalescence events that occurred 3 kpc away with a SNR of about 10. The recorded variation of expected binary range for coalescence of 0.5 $M_\odot$, 1.4 $M_\odot$, and 10 $M_\odot$ equal-mass binary systems is shown in Fig. 9, for a time stretch of about 24 h of observation. There was no significant sensitivity decrease during this period, and the important result was that there was no day-night effect on the trend as was strongly experienced at the Tokyo site. This shows that the antenna was kept operable in the daytime as well as in the nighttime, which means that human activities in the daytime had almost no effect on the antenna at this site. The distribution of the binary range value for some stable period shows good Gaussianity, with a relatively small standard deviation. If we define a ''sensitive-operation'' duty cycle, which allows a 3 dB decrease of the SNR from the center value, instead of the ''in-lock operation'' duty cycle, it becomes about 90% for each mass binary systems.

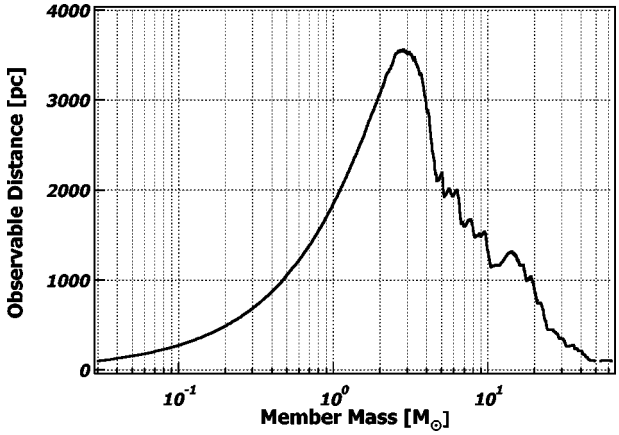

FIG. 8. The expected binary range of the gravitational wave signals from equal mass binary inspirals with SNR=10 by matched filtering method. For simplicity, optimal source direction and polarization are assumed.

VI. CONCLUSION

The prototype laser interferometer gravitational wave antenna LISM with an arm length of 20 m was moved into a

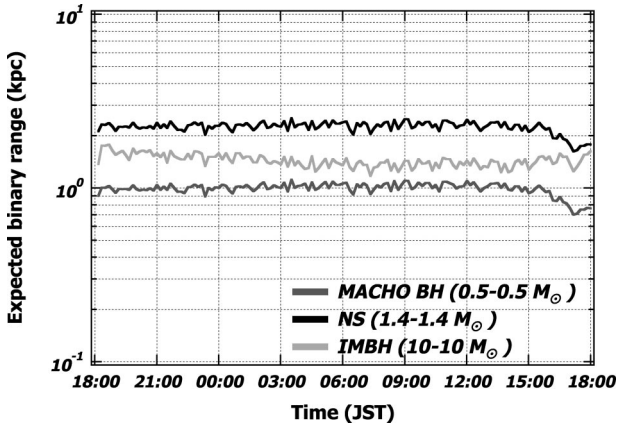

FIG. 9. The stability of the expected binary range for 0.5, 1.4, and 10 solar mass binary systems for 24 h. There seemed to be no significant decrease in each binary range, which means that the LISM antenna was stably operated to keep initial spectral sensitivity. Another emphasis should be on the fact that there was no day-night effect, which is the case at the Tokyo site because of various human activities in the daytime.

deep underground laboratory, a first for gravitational wave observatories, and a long-term observational run was performed. The goal of this project was to confirm that the laser interferometer can operate stably and provide high-quality data, making the most of the stable environment in the underground laboratory. The interferometer sensitivity achieved was $1\times10^{-18}\mathrm{m}/\sqrt{\mathrm{Hz}}$ around 800 Hz in displacement, which corresponds to $5\times10^{-20}/\sqrt{\mathrm{Hz}}$ in strain. At higher frequencies, above that floor sensitivity, LISM was quantum noise limited by shot noise. With this sensitivity spectrum, LISM can detect gravitational wave events emitted from coalescence of 1.4–1.4 $M_{\odot}$ equal-mass binary systems a few kpc away by matched filtering analysis with a SNR of 10. The operational duty cycle of the interferometer exceeded 99.8% owing to the stable, low-disturbance environment and the self-recovering automation systems. If we adopt the expected SNR of the matched filtering analysis as an index for stability of the interferometer sensitivity, this SNR duty cycle was about 90%. This means that the interferometer sensitivity was kept within a 3 dB window for 90% of the observational period. According to these results, we conclude that the laser interferometer gravitational wave antenna was operated stably enough for a long-term observational run, and the underground environment is suitable as a gravitational wave antenna site.

ACKNOWLEDGMENTS

The authors are grateful to the LISM Collaboration for their assistance and also would like to thank A. Rüdiger and P. Beyersdorf for valuable discussion. The authors would also like to thank R. Savage for providing the LHO seismic noise spectrum data. This research was partially supported by the Ministry of Education, Science, Sports and Culture, Grant-in-Aid for Scientific Research (A), 11304013, 1999.

[1] A. Abramovici, W.E. Althouse, R.W.P. Drever, Y. Gürsel, S. Kawamura, F.J. Raab, D. Shoemaker, L. Sievers, R.E. Spero, K.S. Thome, R.E. Vogt, R. Weiss, S.E. Whitcomb, and M.E. Zucker, Science **256**, 325 (1992).
[2] B. Barish and R. Weiss, Phys. Today **52**(10), 44 (1999).
[3] C. Bradaschia *et al.*, Nucl. Instrum. Methods Phys. Res. A **289**, 518 (1990).
[4] F. Acernese *et al.*, Class. Quantum Grav. **19**, 1421 (2002).
[5] K. Danzmann *et al.*, Internal Rep. MPQ Max-Planck-lnstitut für Quantenoptik, Garching, Germany, Vol. 190 (1994).
[6] K. Danzmann, in *First E. Amaldi Conference on Gravitational Wave Experiments*, edited by E. Coccia, G. Pizzella, and F. Ronga (World Scientific, Singapore, 1994), pp. 100–111.
[7] B. Willke *et al.*, Class. Quantum Grav. **19**, 1377 (2002).
[8] K. Tsubono, in *First E. Amaldi Conference on Gravitational Wave Experiments* (Ref. [6]), pp. 112–114.
[9] M. Ando *et al.*, Class. Quantum Grav. **19**, 1409 (2002).
[10] TAMA Collaboration, M. Ando *et al.*, Phys. Rev. Lett. **86**, 3950 (2001).
[11] V. Kalogera, R. Narayan, D.N. Sperge, and J.H. Taylor, Astrophys. J. **556**, 340 (2001).
[12] C. Kim, V. Kalogera, and D.R. Lorimer, Astrophys. J. **584**, 985 (2003).
[13] M. Burgay, N. D'Amico, A. Possenti, R.N. Manchester, A.G. Lyne, B.C. Joshi, M.A. McLaughlin, M. Kramer, J.M. Sarkissian, F. Camilo, V. Kalogera, C. Kim, and D.R. Lorimer, Nature (London) **426**, 531 (2003).
[14] M. Ohashi, M.-K. Fujimoto, T. Yamazaki, M. Fukushima, A. Araya, and S. Telada, in *Proceedings of the Seventh Marcel Grossmann Meeting on General Relativity*, edited by Robert T. Jantzen and G. MacKeiser (World Scientific, Singapore, 1996), pp. 1370–1371.
[15] A. Araya, N. Mio, K. Tsubono, K. Suehiro, S. Telada, M. Ohashi, and M.-K. Fujimoto, Appl. Opt. **36**, 1446 (1997).
[16] S. Telada, K. Suehiro, S. Sato. M. Ohashi, M.-K. Fujimoto, and A. Araya, in *Proceedings of the 1st TAMA International Workshop on Gravitational Wave Detection*, edited by K. Tsubono, M.-K. Fujimoto, and K. Kuroda (Universal Academy Press, Inc., Tokyo, 1996), pp. 349–351.
[17] S. Sato, M. Ohashi, M.-K. Fujimoto, M. Fukushima, K. Waseda, S. Miyoki, N. Mavalvala, and H. Yamamoto, Appl. Opt. **39**, 4616 (2000).
[18] H. Takahashi *et al.*, Phys. Rev. D, http://arxiv.orglabs/gr-qc/0403088.
[19] Y. Fukuda *et al.*, Phys. Rev. Lett. **81**, 1562 (1998).
[20] K. Kuroda *et al.*, Int. J. Mod. Phys. D **8**, 557 (1999).
[21] K. Kuroda *et al.*, Class. Quantum Grav. **20**, S871 (2003).
[22] M. Zucker, in *Proceedings of the 6th Marcel Grossmann Meeting on General Relativity, Kyoto, Japan* (World Scientific, Singapore, 1991).
[23] S. Sato, S. Miyoki, M. Ohashi, M.-K. Fujimoto, T. Yamazaki, M. Fukushima, A. Ueda, K. Ueda, K. Watanabe, K. Nakamura, K. Etoh, N. Kitajima, K. Ito, and I. Kataoka, Appl. Opt. **38**, 2880 (1999).
[24] R.W.P. Drever, J.L. Hall, F.V. Kowalski, J. Hough, G.M. Ford, A.J. Munley, and H. Ward, Appl. Phys. B: Photophys. Laser Chem. **31**, 97 (1983).
[25] S. Kawamura, A. Abramovici, and M.E. Zucker, Rev. Sci. Instrum. **68**, 223 (1997).
[26] Y. Tamura, T. Sato, M. Ooe, and M. Ishigro, Geophys. J. Int. **104**, 507 (1991).
[27] M. Ando, internal document (2001).
[28] H. Tagoshi *et al.*, Phys. Rev. D **63**, 062001 (2001).
[29] D. Shoemaker *et al.*, *The ligo observatory environment* (2001), LIGO technical document LIGO-T010074-03-D http://www.ligo.caltech.edu/docs/T/T010074-03/T010074-03.pdf.